Acta Montanistica Slovaca
ISSN 1335-1788
actamont.tuke.sk

Using color-only vegetation indexes to remove vegetation from otherwise mostly mono-material point clouds

Martin ŠTRONER[1], Rudolf URBAN[2], Tomáš SUK[3] and Vilém KOLÁŘ[4]*

Authors' affiliations and addresses:
[1] Department of Special Geodesy, Faculty of Civil Engineering, Czech Technical University in Prague, Thákurova 7, 166 36 Prague 6, Czech Republic
e-mail: martin.stroner@fsv.cvut.cz

[2] Department of Special Geodesy, Faculty of Civil Engineering, Czech Technical University in Prague, Thákurova 7, 166 36 Prague 6, Czech Republic
e-mail: rudolf.urban@fsv.cvut.cz

[3] Department of Special Geodesy, Faculty of Civil Engineering, Czech Technical University in Prague, Thákurova 7, 166 36 Prague 6, Czech Republic
e-mail: tomas.suk@fsv.cvut.cz

[4] Department of Special Geodesy, Faculty of Civil Engineering, Czech Technical University in Prague, Thákurova 7, 166 36 Prague 6, Czech Republic
e-mail: vilem.kolar@fsv.cvut.cz

***Correspondence:**
Martin Štroner, Department of Special Geodesy, Faculty of Civil Engineering, Czech Technical University in Prague, Thákurova 7, 166 36 Prague 6, Czech Republic
tel.: +420-22435-4781
e-mail: martin.stroner@fsv.cvut.cz

Funding information:
Grant Agency of CTU in Prague
SGS21/053/OHK1/1T/11
Technology Agency of the Czech Republic
CK03000168

Acknowledgment:
This research was funded by the GA of CTU in Prague - grant SGS22/046/OHK1/1T/11 "Optimization of acquisition and processing of 3D data for purpose of engineering surveying, geodesy in underground spaces and 3D scanning "and by Technology Agency of the Czech Republic – grant number CK03000168 "Intelligent methods of digital data acquisition and analysis for bridge inspections ".

How to cite this article:
Štroner, M., Urban, R., Suk, T. and Kolář, V. (2022). Using color-only vegetation indexes to remove vegetation from otherwise mostly mono-material point clouds. *Acta Montanistica Slovaca*, Volume 27 (4), 1089-1101

DOI:
https://doi.org/10.46544/AMS.v27i4.20

Abstract
Point clouds are now a standard way of describing objects in many engineering disciplines, whether they are man-made objects such as structures, buildings, or various types of structures. Commonly used methods of acquiring such data include ground, UAV, or even aerial photogrammetry, followed by terrestrial, UAV, and aerial scanning. After measurement (by the scanner) or calculation (from photogrammetry), the point cloud goes through extensive processing that essentially transforms the unordered mass of points into a usable data set. One of the important steps is removing points representing obstructing objects and features, including vegetation in particular. Here, many filtering methods based on different principles are available and suitable for application to different scenes.
This paper presents a new method of filtering point clouds based on the visible spectrum color principle using vegetation indexes determined from RGB system colors only. Since each sensor has to some extent, an individual interpretation of the colors, it cannot be assumed to determine specific boundaries of what is and is no longer vegetation. Therefore, it was proposed to use means clustering to simplify the operator's work. The method was also designed in such a way that the entire evaluation could be implemented in the freely available CloudCompare software.
The procedure was tested on three different sites with different terrain and vegetation characteristics showing, which demonstrated the applicability of this method to data where the color information (green) uniquely identifies vegetation. The selected vegetation filters ExG, ExR, ExB, and ExGr were tested, where ExG was the best. K-means clustering helps an operator to distinguish more easily between vegetation and the rest of the point cloud without compromising the quality of the result. The method is practically implementable using the freely downloadable and usable CloudCompare software.

Keywords
Point cloud; vegetation index; vegetation filtering

Introduction

Point clouds are now a standard way of describing objects in many engineering disciplines, whether they are man-made objects such as structures, buildings, or various types of structures (e. g. bridges (Erdélyi, Kopáčik, & Kyrinovič, 2020), buildings (Kovanič et al, 2021)). Commonly used methods of acquiring such data include ground (Křemen, 2020), UAV (Rybansky, 2022) (Urban, Štroner, & Kuric, 2020) (Blišťan et al., 2019), or even aerial photogrammetry (Blišťan et al., 2016) (here the Structure from Motion (SfM) method is absolutely predominant), followed by terrestrial (Koska & Křemen, 2013), UAV (Jon, Koska & Pospíšil, 2013) and aerial scanning (Kovanič et al., 2021).

The point cloud, after measurement (by the scanner) or calculation (from photogrammetry), goes through processing (Pavelka et al., 2019) that essentially transforms the unordered mass of points into a usable data set. One of the important steps is removing points representing obstructing objects and features, including vegetation in particular (Braun et al., 2022). Here, many filtering methods based on different principles are available and suitable for application to different scenes. Filters can be divided into geometric (slope-based (Vosselman, 2000) (Sithole, 2001) (Susaki, 2012), interpolation-based (Kraus & Pfeifer, 1998) (Axelsson, 2000) (Kobler et al., 2007), morphological (Keqi Zhang et al., 2003) (Pingel, Clarke, & McBride, 2013) (Li, 2013), statistical (Bartels & Wei, 2006)), segmentation-based (Im, Jensen, & Hodgson, 2008) (Zhang, Lin, & Ning, 2013) (Tovari & Pfeifer, 2005) (Vosselman, Coenen, & Rottensteiner, 2017), machine learning-based (Rizaldy et. el, 2018) (Zhang, Hu, Dai, & Qu, 2020), and hybrid and other filters (e.g., (Buján, Cordero, & Miranda, 2020), (Zhang et al., 2016). These filters are suitable for point clouds where the points representing necessary objects are distinguishable from unnecessary ones through spatially manifested properties, be it a difference in slope, data structure, or something else. Furthermore, most of these filters were developed in response to the processing of point clouds taken by airborne lidars, whose data are relatively low in detail and are mainly intended to obtain a digital terrain model (Moudrý et al., 2013) (Moravec et al., 2017) (Blistanova et al 2015). It is only recently that filters specialized (or at least suitable) for technical applications where the clouds are dense, i.e., with resolution in the units of centimeters (or better) and with similar accuracy (Štroner, Urban & Línková, 2022) (Štroner, Urban, Lidmila, Kolář, & Křemen, 2021) have been developed.

However, all of these filters are only functional under the basic assumption - necessary and obstructing points can only be separated based on the spatial arrangement. If this is not the case, they are completely powerless. Examples include dense low shrubbery in rugged areas where earthworks are carried out, on rock faces, in opencast mines, etc. The spatial granularity of these stands is similar to or even lower than that of the terrain. They do not stand out from it in any way and are, therefore, geometrically indistinguishable. Nevertheless, the processor can distinguish them at a glance on the basis of color. The way color is commonly expressed through the Red, Green, and Blue (RGB) components does not allow the selection of what is green as a human would, and so some other expression must be used. Vegetation indexes that also use invisible spectra of electromagnetic radiation (such as NDVI) can be used to express the amount of green, but this requires special sensors (and can only be used for photogrammetric methods). Thus, either other color expression systems (e.g., HSI - Hue, Saturation, Intensity) or vegetation indexes using only visible radiation captured by RGB sensors (which is possible for all the technologies described) are offered.

This paper presents a new method of filtering point clouds based on the visible spectrum color principle using vegetation indexes determined from RGB system colors only. Since each sensor has to some extent, an individual interpretation of the colors, it cannot be assumed to determine specific boundaries of what is and is no longer vegetation. Therefore, a simple point cloud color segmentation system (using the k-means clustering algorithm, see https://en.wikipedia.org/wiki/K-means_clustering) was proposed to make it easier for the operator to determine the boundary between vegetation and the rest of the surfaces. This converts a virtually continuous value domain into a value domain with only discrete values. The testing also includes determining the effect of the number of color clusters on the quality of the result. So far, the method aims to identify points with green color. Although vegetation is not only green but also woody but in terms of point cloud filtering, these features are generally much fewer.

Materials and Methods

The proposed method is based on the simple assumption that instead of the operator manually removing the vegetation points based on the subjective evaluation according to the color he sees on the screen, according to a clear mathematical rule, a score number is calculated for each cloud point, based on which it is decided whether the point is removed or not.

The key is, of course, the selection of a suitable vegetation index, of which there is a plethora in the literature, and they are aimed at solving different tasks. Thus, the idea of using vegetation indexes is not new. However, they have always been applied to image data so far, especially in applications of greenness assessment in image data

for agricultural purposes, e.g., in (Änäkkälä, Lajunen, Hakojärvi, & Alakukku, 2022) or in (Guijarro et al., 2011) and (D. M. Woebbecke, G. E. Meyer, K. Von Bargen, & D. A. Mortensen, 1995).

Proposed filtration procedure

The proposed method consists of a few simple steps:

1. Calculation of the vegetation index (VI) for each point of the cloud.
2. Limiting the range of the vegetation index for the cloud so that outliers do not unnecessarily increase the range.
3. Segmenting the cloud VI into k groups.
4. Choosing a boundary for vegetation identification.
5. Vegetation filtering.

The calculation can be performed in mathematical software such as Matlab or Scilab. However, the procedure has been developed for an easy practical application that is entirely executable in the CloudCompare software environment; the current version 2.12.4 was used for testing. After the point cloud is loaded into the program, it is necessary to export the colors of the points into scalar fields named R, G, and B (using the Edit/Colors/Convert to scalar field function). The specific vegetation index value is then calculated using the Edit/Scalar fields/ Arithmetics function. The histogram (Edit/Scalar fields/Show histogram) can be used to find the appropriate range boundaries. A boundary corresponding to a cumulative probability of about 0.1% on the left side and the same for the right side can be recommended. These selected values are set as outliers in the SF display params field for the saturation boundaries (bottom part). Then you need to set the color gamut to Grey and import the scalar field thus displayed into color (Edit/Scalar Fields/Convert to RGB).

Then the function Plugins/Calorimetric segmenter/Kmeans Clustering is used, where the number of resulting colors k and the maximum number of iterations are set (more does not matter, the converging calculation usually terminates much earlier than the defined value, i.e., it is recommended to set 100). The function adjusts the colors, which are then exported again to the scalar field, just the composite channel ((R+B+G)/3). This scalar field then contains the segmented colors at a maximum of k. The original true colors are returned to the point cloud using the Edit/Colors/From Scalar fields function (from the originally exported R, G, and B channels). You need to set a maximum range for each R, G, and B channel and a fixed value of 255 for the Alpha channel.

Data for testing

To test the method, its setup, and the vegetation indexes used, the following data were selected to correspond to the intended use, i.e., to such point clouds where vegetation is not part of the search surface, such as rock formations, mining areas, earthwork, and landscaping works. Data 1 (Fig. 1) is from a stone rubble field in the High Tatras; the selected cloud has an area of 4800 m^2 and consists of 1 554 452 points.

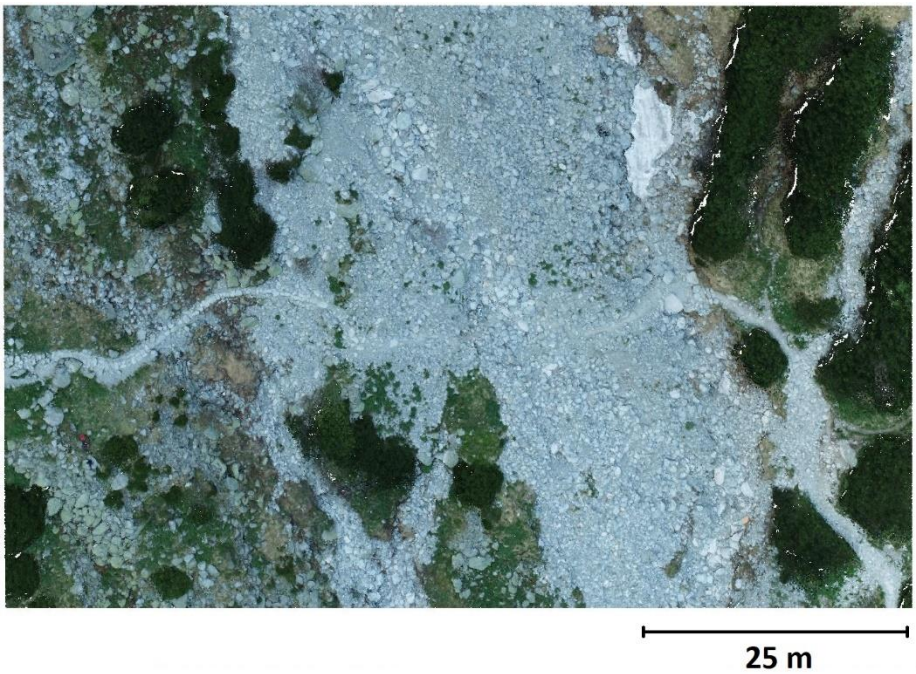

Fig. 1. Data 1 point cloud – a stone field with surrounding low alpine vegetation

The average density is 264 points per m^2, i.e., the distance between adjacent points is about 0.06 m.

Data 2 (Fig. 2) is from a vertical stone wall of a yellow-brown hue, a railway cut, where there are clumps of grass to be removed. The cloud has 1,594,685 points, and the area of the rock is 242 m^2. The average density is 3550 points per m^2, i.e., the distance between adjacent points is about 0.02 m.

Fig. 2. Data 2 point cloud – almost vertical rock wall with small clumps of vegetation

Data 3 is from an area of ground works where dense ground shrubs have grown up, preventing detection of the ground surface by non-contact methods. The cloud has 1 688 681 points and covers an area of 3 383 m^2. The average density is 480 points per m^2, i.e., the distance between adjacent points is about 0.05 m.

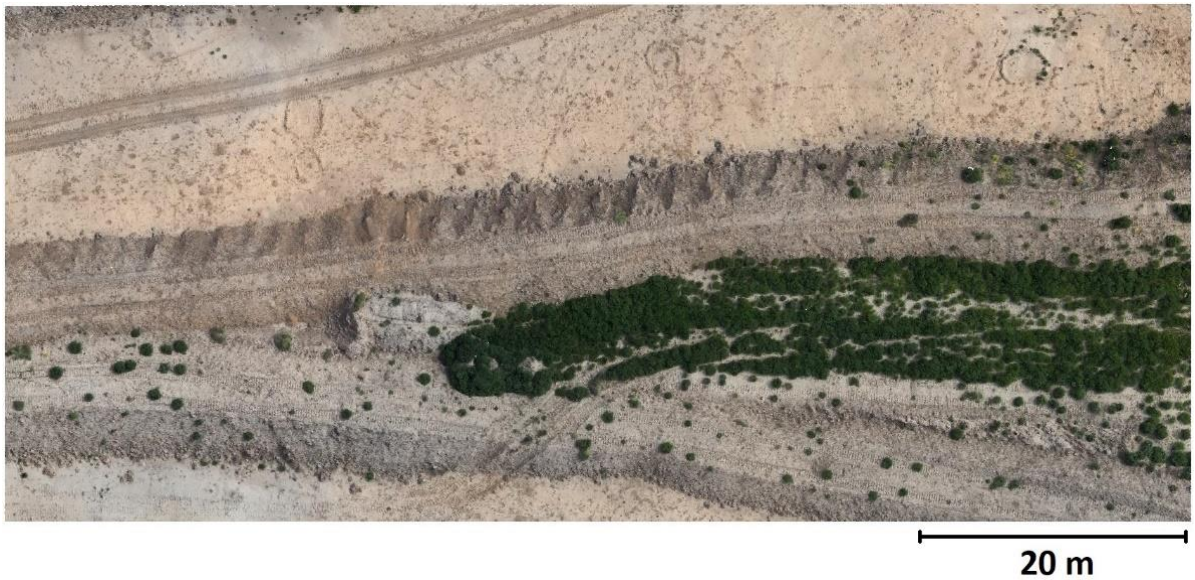

Fig. 3. Data 3 point cloud – an area of landscaping with vegetation - dense bushes

Vegetation indexes tested

Vegetation indexes are given in Tab. 1. Here R, G, and B are the point colors in the range 0 - 255, and r, g, and b are the normalized color values:

$$r = R/(R+G+B) \quad (1)$$
$$g = G/(R+G+B) \quad (2)$$
$$b = B/(R+G+B) \quad (3)$$

Tab. 1. Summary of vegetation indexes used

Name	Abbreviation	Formula	Reference
Excess Green	ExG	ExG = 2g – r – b	(Woebbecke, 1995)
Excess Red	ExR	ExR = 1.4r – g	(Meyer, 1999)
Excess Blue	ExB	ExB = 1.4b – g	(Guijarro, 2011)
Excess Green	ExGr	ExGr = ExG – ExR	(Camargo Neto, 2004)

Testing methodology

Each data was filtered using each of the indexes listed (ExG, ExR, ExB, ExGr) with the data separated manually without adjustment and further with K-means segmentation into 2, 3, 4, 5, 10, 15, 20, 50, and 100 steps. For each data, an etalon was created by a human operator against which the variants were evaluated.

The first characteristic used is the type I error and type II error of vegetation point identification. Type I error refers to points that should have been identified as green and mistakenly were not (sometimes also called false negative rate). Type II error then indicates points that were incorrectly identified as green (false positive rate). Both errors are expressed as percentages in this paper, where 100% is the number of vegetation points according to the etalon. In addition, established binary classification quality characteristics were calculated, namely the well-known f-score (according to (Fawcett, 2006)), accuracy, and balanced accuracy (according to https://en.wikipedia.org/wiki/Evaluation_of_binary_classifiers, 1.10.2022), the calculation is shown in Tab. 2.

Tab. 2 Overview of quality characteristics used

Characteristics	Abbreviation	Calculation
Type I error	I	I = FN/(TP+FN)
Type II error	II	II = FP/(TP+FN)
Total error	TE	TE = I + II
F-score	FS	FS = 2TP/(2TP+FP+FN)
Accuracy	AC	AC = (TP+TN)/(TP+TN+FP+FN)
Balanced accuracy	BA	BA = (TPR+TNR)/2; TPR = TP/(TP+FN); TNR = TN/(TN+FP)

Since this is a binary classification, the data are divided into two basic parts - positive P and negative N (in the case of cloud classification, these are the sets of vegetation points and other points). Furthermore, a successful classification is denoted as true (T) and an unsuccessful one as false (F). Thus, e.g., TP denotes true positive; in the case of the point cloud classification reported here, these are points correctly classified as vegetation, then, e.g., FP denotes false positive, i.e., points incorrectly identified as vegetation points, TN points correctly classified as other points, etc.

Results

The results of the testing are shown in the following tables. In particular, the TE variable - the total proportion of misidentified points - can be used for the simplest interpretation. Furthermore, the quality is also well expressed by BA - the quality of the identification of both vegetation and non-vegetation points.

Data 1 represents a scene consisting of grey stones, grass, dirt, and dwarf mountain pine trees. All the characteristics of the quality of the greenness identification show that of the vegetation indexes tested, ExG appears to be the most suitable, with ExGr as the second best, then ExB, and visibly the worst ExR. When evaluating the effect of the number of clusters k, it is clear that except for the minimum values (2-4), the results do not differ much. It may seem illogical that when calculating without simplifying to k clusters (k = full), the results are worse in some cases. This is because the subtle value shift is difficult for the operator to evaluate, manifesting itself differently at different points in the cloud.

It must also be taken into consideration that the etalon created for the assessment is very difficult to create, the boundary of the green color indicating vegetation is not sharp, the data comes from sensors with limited resolution, and of course, each operator has a different perception of color, and the different color display on different screens contributes to the uncertainty of the result.

From the point of view of the interpretation of the results, it is worth adding that out of about 1.5 million points, about 420 thousand points are identified as vegetation.

Data 2 has a different color background; the rock is mostly yellow-brown. The vegetation identification here fails dramatically with vegetation indexes ExR and ExB, where the sum of misidentified TE points reaches higher tens of percent. Again, ExG performs very well here, while ExGr is significantly worse. Out of about 1.5 million points, only about 54 thousand points are identified as vegetation. Therefore, the percentages are significantly different in some characteristics.

The results for Data 3 replicate the previous results, with ExB and ExR achieving about the same results, ExGr being visibly better and ExG the best. Of the approx. 1.4 million points, approx. 254 thousand points are identified as vegetation ones.

Tab. 1 Testing results – Data 1

V. Index	k	I [%]	II [%]	TE [%]	f-score [%]	BA [%]	ACC [%]
ExG	2	20.28	0.00	20.28	88.72	89.86	94.52
	3	0.07	8.63	8.70	95.83	98.37	97.65
	4	23.16	0.00	23.16	86.91	88.42	93.74
	5	0.37	0.40	0.77	99.61	99.74	99.79
	10	3.27	0.26	3.52	98.21	98.32	99.05
	15	0.37	0.40	0.77	99.61	99.74	99.79
	20	5.10	0.19	5.29	97.29	97.42	98.57
	50	0.09	4.70	4.78	97.66	99.09	98.71
	100	0.00	1.95	1.95	99.03	99.64	99.47
	Full	0.09	5.12	5.20	97.46	99.01	98.59
ExR	2	27.21	0.50	27.71	84.01	86.30	92.51
	3	34.28	2.28	36.55	78.24	82.44	90.11
	4	22.35	9.18	31.53	83.12	87.12	91.47
	5	32.41	2.77	35.18	79.35	83.28	90.49
	10	24.83	6.76	31.59	82.64	86.33	91.46
	15	21.78	10.12	31.90	83.06	87.23	91.37
	20	22.35	9.18	31.53	83.12	87.12	91.47
	50	20.99	11.17	32.17	83.09	87.43	91.30
	100	20.99	11.17	32.17	83.09	87.43	91.30
	Full	20.89	11.32	32.21	83.08	87.46	91.29
ExB	2	11.64	7.40	19.03	90.28	92.81	94.85
	3	2.48	32.12	34.59	84.94	92.81	90.65
	4	20.14	2.46	22.60	87.60	89.47	93.89
	5	5.39	19.00	24.39	88.58	93.78	93.41
	10	8.71	11.18	19.89	90.18	93.57	94.62
	15	20.14	2.46	22.60	87.60	89.47	93.89
	20	9.79	9.54	19.33	90.32	93.34	94.77
	50	16.79	3.77	20.56	89.00	90.91	94.44
	100	8.71	11.18	19.89	90.18	93.57	94.62
	Full	17.64	3.39	21.03	88.68	90.55	94.31
ExGr	2	22.82	0.05	22.87	87.10	88.58	93.82
	3	2.64	10.70	13.34	93.59	96.70	96.39
	4	18.35	0.15	18.50	89.82	90.80	95.00
	5	1.57	15.90	17.47	91.85	96.27	95.28
	10	5.82	4.24	10.06	94.93	96.31	97.28
	15	1.88	13.92	15.80	92.55	96.48	95.73
	20	5.82	4.24	10.06	94.93	96.31	97.28
	50	1.88	13.92	15.80	92.55	96.48	95.73
	100	5.22	5.04	10.27	94.86	96.45	97.22
	Full	6.31	3.76	10.07	94.90	96.15	97.28

Tab. 4 Testing results – Data 2

V. Index	k	I [%]	II [%]	TE [%]	f-score [%]	BA [%]	ACC [%]
ExG	2	8.42	0.60	9.03	95.30	95.78	99.69
	3	15.99	0.33	16.33	91.14	92.00	99.45
	4	21.29	0.23	21.52	87.97	89.35	99.27
	5	23.73	0.20	23.93	86.44	88.13	99.19
	10	0.00	9.26	9.26	95.57	99.84	99.69
	15	0.00	32.13	32.13	86.16	99.44	98.91
	20	26.11	0.16	26.27	84.91	86.94	99.11
	50	7.38	0.64	8.02	95.85	96.30	99.73
	100	0.00	7.25	7.25	96.50	99.87	99.75
	Full	0.91	1.01	1.93	99.04	99.53	99.93
ExR	2	0.28	663.58	663.86	23.10	88.20	77.46
	3	16.97	41.78	58.75	73.87	90.78	98.01
	4	37.05	8.44	45.50	73.45	81.33	98.46
	5	2.89	203.33	206.22	48.50	94.98	93.00
	10	7.10	104.34	111.44	62.51	94.62	96.22
	15	12.94	58.48	71.42	70.91	92.50	97.58
	20	14.84	49.48	64.32	72.59	91.71	97.82
	50	26.96	19.34	46.30	75.93	86.18	98.43
	100	16.97	41.78	58.75	73.87	90.78	98.01
	Full	59.25	0.88	60.13	57.55	70.36	97.96
ExB	2	9.21	1361.53	1370.75	11.70	71.47	53.46
	3	23.71	609.87	633.59	19.41	77.43	78.49
	4	41.43	223.58	265.02	30.65	75.35	91.00
	5	45.51	174.49	220.00	33.13	74.18	92.53
	10	83.17	0.00	83.17	28.81	58.42	97.18
	15	58.77	56.37	115.15	41.73	69.62	96.09
	20	74.61	0.02	74.63	40.49	62.70	97.47
	50	74.61	0.02	74.63	40.49	62.70	97.47
	100	73.85	0.02	73.87	41.45	63.07	97.49
	Full	69.94	0.12	70.06	46.19	65.03	97.62
ExGr	2	19.01	0.58	19.59	89.21	90.49	99.33
	3	27.73	0.14	27.87	83.84	86.13	99.05
	4	31.93	0.08	32.01	80.96	84.03	98.91
	5	31.93	0.08	32.01	80.96	84.03	98.91
	10	9.90	3.98	13.88	92.85	94.98	99.53
	15	12.60	2.24	14.84	92.17	93.66	99.50
	20	15.68	1.16	16.84	90.92	92.14	99.43
	50	4.25	15.19	19.44	90.78	97.61	99.34
	100	6.33	8.83	15.17	92.51	96.68	99.48
	Full	13.75	1.79	15.54	91.74	93.09	99.47

Tab. 5 Testing results – Data 3

V. Index	k	I [%]	II [%]	TE [%]	f-score [%]	BA [%]	ACC [%]
ExG	2	20.16	0.00	20.16	88.79	89.92	96.96
	3	5.74	0.00	5.75	97.04	97.13	99.13
	4	0.00	5.92	5.92	97.12	99.47	99.11
	5	0.00	0.77	0.77	99.61	99.93	99.88
	10	0.00	12.87	12.87	93.96	98.86	98.06
	15	7.39	0.00	7.39	96.16	96.31	98.89
	20	0.00	0.03	0.03	99.98	100.00	100.00
	50	0.00	2.37	2.37	98.83	99.79	99.64
	100	0.00	3.19	3.19	98.43	99.72	99.52
	Full	1.50	0.02	1.51	99.24	99.25	99.77
ExR	2	21.57	0.01	21.58	87.91	89.21	96.74
	3	27.29	0.00	27.29	84.20	86.35	95.88
	4	14.84	0.09	14.94	91.94	92.57	97.75
	5	18.66	0.02	18.68	89.70	90.67	97.18
	10	12.23	0.29	12.52	93.34	93.86	98.11
	15	5.09	3.40	8.49	95.72	97.15	98.72
	20	3.37	9.23	12.60	93.88	97.50	98.10
	50	14.19	0.12	14.31	92.30	92.89	97.84
	100	4.78	4.39	9.18	95.40	97.22	98.62
	Full	10.03	0.60	10.63	94.42	94.93	98.40
ExB	2	22.71	0.08	22.79	87.15	88.64	96.56
	3	27.95	0.03	27.98	83.74	86.02	95.78
	4	16.81	0.26	17.07	90.69	91.57	97.42
	5	9.53	1.74	11.27	94.14	95.08	98.30
	10	8.75	2.15	10.90	94.36	95.43	98.36
	15	5.81	5.40	11.22	94.38	96.61	98.31
	20	16.81	0.26	17.07	90.69	91.57	97.42
	50	7.99	2.70	10.69	94.51	95.76	98.39
	100	4.43	8.53	12.96	93.65	97.03	98.04
	Full	6.13	4.80	10.93	94.50	96.51	98.35
ExGr	2	20.45	0.00	20.45	88.61	89.77	96.92
	3	23.60	0.00	23.60	86.62	88.20	96.44
	4	8.88	0.00	8.88	95.35	95.56	98.66
	5	9.45	0.00	9.45	95.04	95.28	98.57
	10	2.28	0.67	2.94	98.52	98.80	99.56
	15	0.33	5.88	6.21	96.98	99.32	99.06
	20	3.97	0.15	4.12	97.90	98.00	99.38
	50	0.69	3.27	3.96	98.05	99.37	99.40
	100	5.89	0.02	5.91	96.96	97.05	99.11
	Full	4.19	0.12	4.31	97.80	97.90	99.35

Discussion

Filtering vegetation in point clouds using colors or vegetation indexes is a specific technique that is functional according to the above experimental results. However, as with any other procedure, the prerequisite for their functionality is data suitable for their application. This must be respected, and in our opinion, it cannot be expected that this technique can replace, e.g., geometric filters (Anders, Valente, Masselink, & Keesstra, 2019). In fact, it is only filtering the points whose color contains a green tint. Anyway, based on the experiments, it is clear that even with such a narrow selection of vegetation indexes, different features can be detected. In Fig. 4, Data 1 is shown in its original colors (original) and colored by the individual vegetation indexes used.

The main scene is visible in all results, dwarf mountain pine is well recognizable everywhere. The stones as such, or the paths formed by them, are best distinguished on ExB, while ExR distinguishes areas of light brown grass (upper edge on the right). ExG, for example, practically does not distinguish between stones and brown areas (formed by fallen old grass).

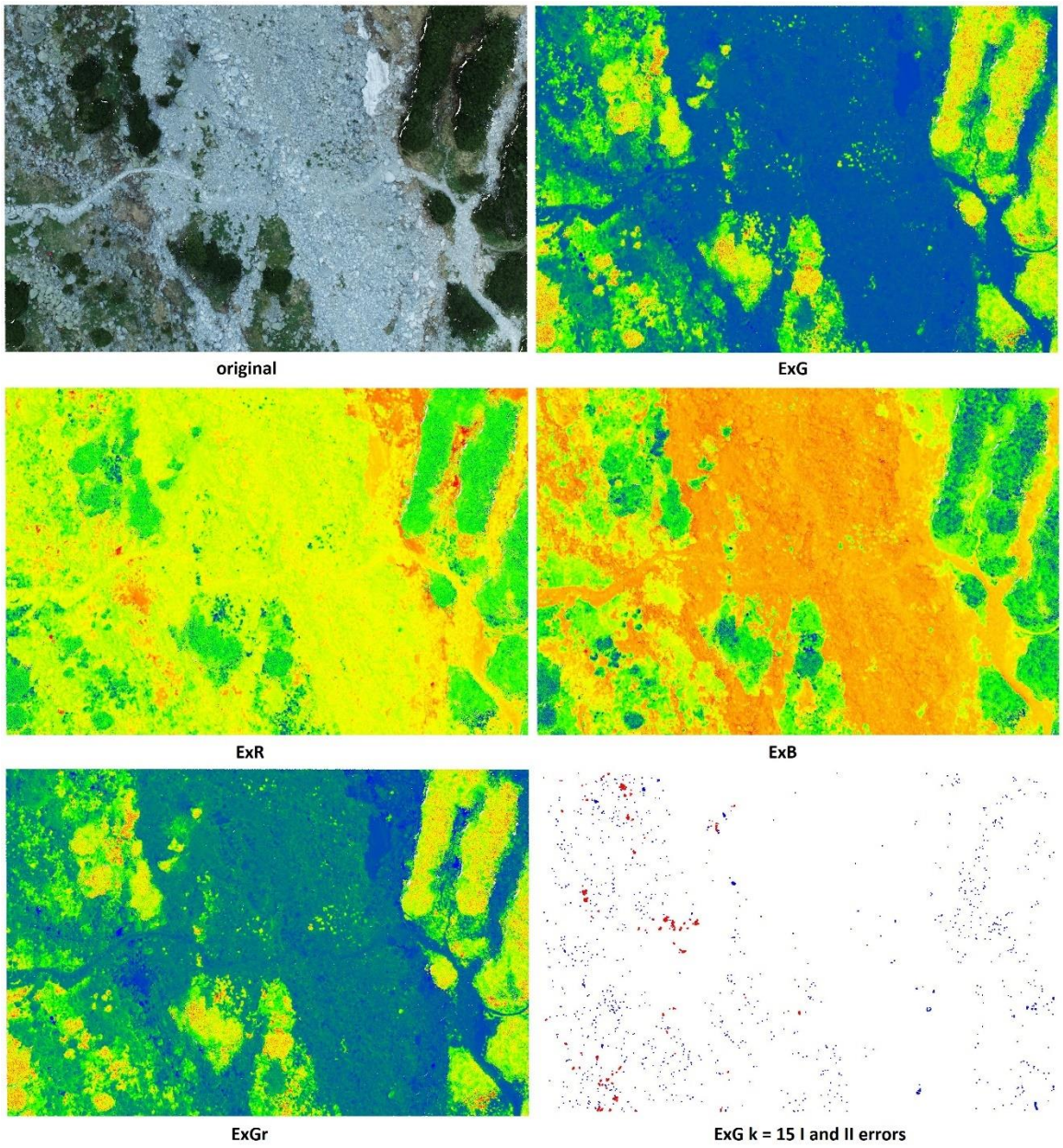

Fig. 4. Data 1 colored according to individual vegetation indexes, and type I (blue) and type II (red) errors for ExG k = 15

Data 2 (Fig. 5) consists of essentially single-colored rock whose color pattern is also created by the illumination - differently tilted surfaces are differently bright, although they are of the same material. ExG again distinguishes only the vegetation, while ExR and ExB accentuate the original colors of the surfaces more. Again, however, the basic identification of vegetation clumps is visible in all images.

Fig. 6 shows similar figures for Data 3. The suitability for this purpose is shown by the virtual absence of the drawing in the blue region for ExG, which is visible for the other indexes.

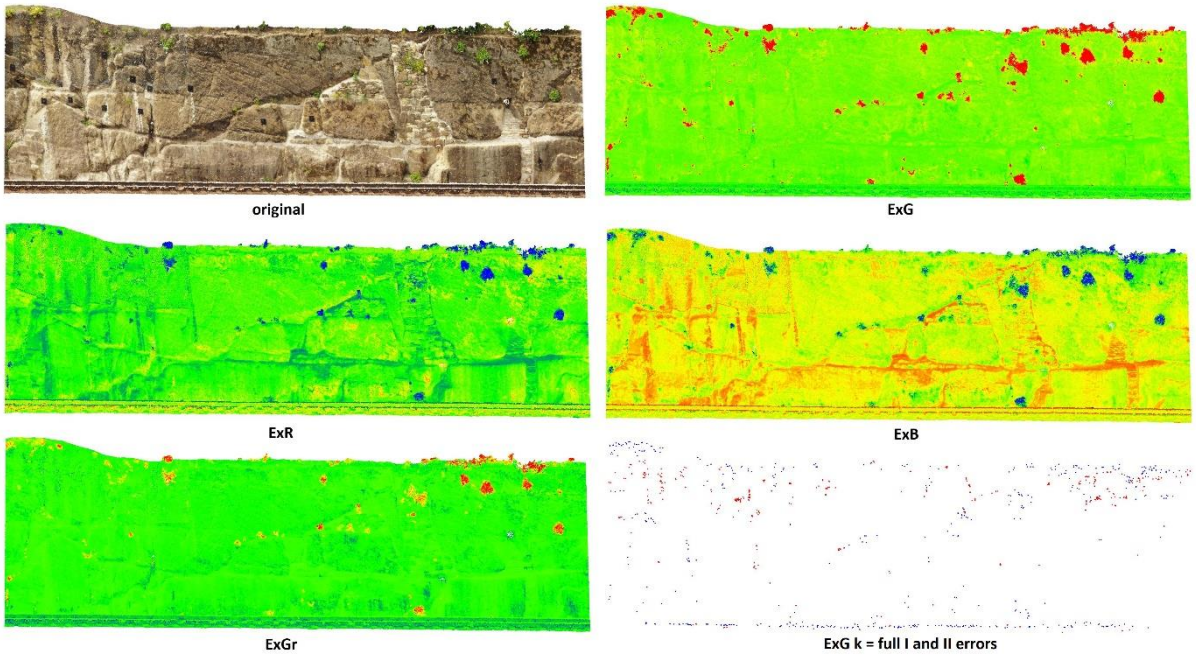

Fig. 5. Data 2 colored according to individual vegetation indexes, and type I (blue) and type II (red) errors for ExG k = full

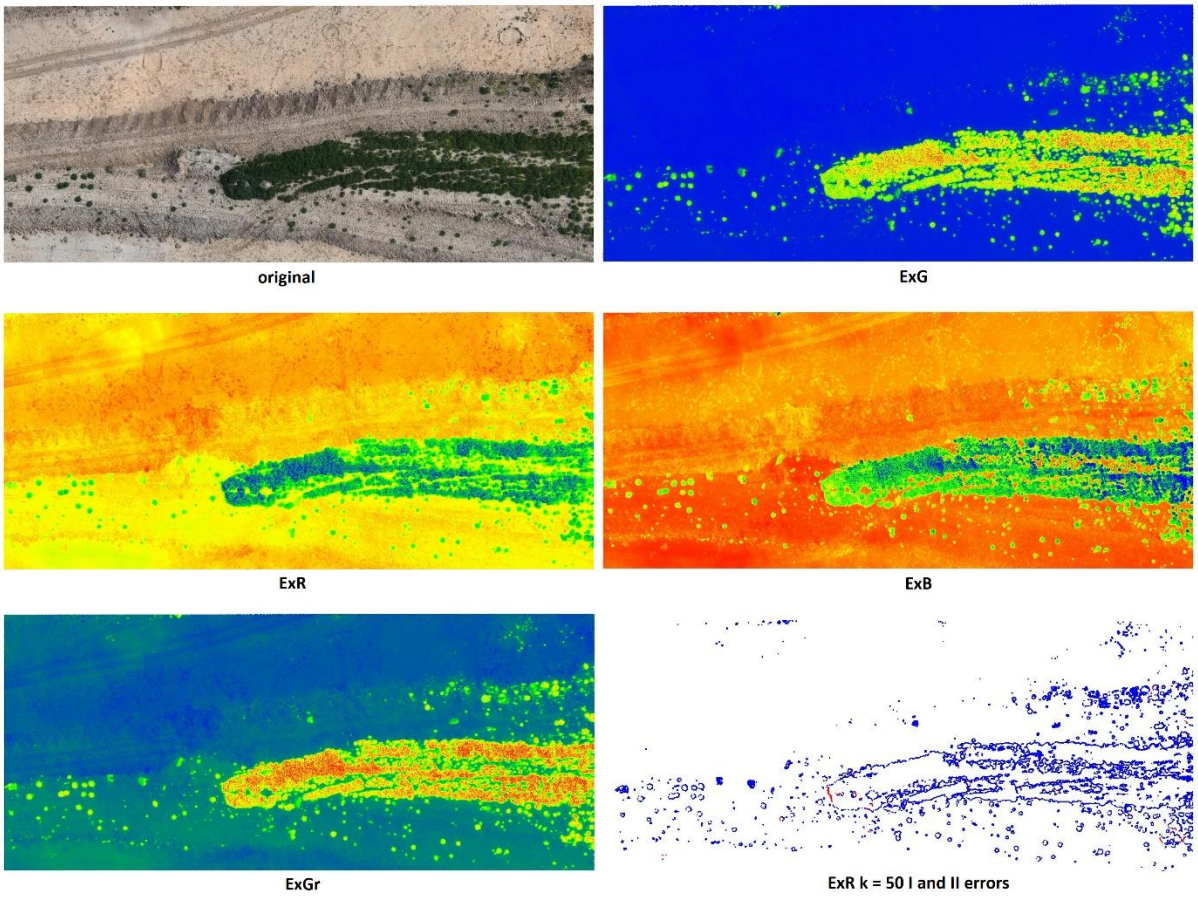

Fig. 6. Data 3 colored according to individual vegetation indexes, and type I (blue) and type II (red) errors for ExR k = 50

As far as the green point identification errors are concerned, it is also worth mentioning here Fig. 4, Fig. 5, and Fig. 6 (always the lower right figure) where specific examples are. Fig. 4 a Fig. 5 illustrate the distribution of misdetected points in very good results, where it can be seen that these are mostly single points and, in fact, on closer examination, it is not possible to say for sure whether the point was correctly evaluated by the algorithm or by a human operator. The case is different in Fig. 6, where the result of the moderately "failed" ExR filter was

selected, where the detection shift is clearly visible, with a kind of wrapper at the different regions defining the vegetation. It is a boundary setting when the detection boundary is further shifted; the vegetation starts to mix with other points.

As a result of the testing, it is found that the match with the human operator's work is best for the vegetation index ExG, the remaining indexes have different properties, and it may be that in different scenes with different materials and therefore, different colors, it may be possible to detect additional feature points to detect the necessary information.

Conclusions

This paper presents a proposed method for filtering vegetation from point clouds based on vegetation indexes determined from RGB color information only. A test is performed to demonstrate the applicability of this method to data where the color information (green) uniquely identifies vegetation. The selected vegetation filters ExG, ExR, ExB, and ExGr were tested, where ExG was the best. K-means clustering helps an operator to distinguish more easily between vegetation and the rest of the point cloud without compromising the quality of the result. The method is practically implementable using the freely downloadable and usable CloudCompare software. However, when applying the method, it is important to beware of the fact that the image information in mobile or UAV scanners may be significantly spatially shifted (Štroner, Urban, & Línková, 2021).

References

Änäkkälä, M., Lajunen, A., Hakojärvi, M., & Alakukku, L. (2022). Evaluation of the Influence of Field Conditions on Aerial Multispectral Images and Vegetation Indices. Remote Sensing, 14(19), 4792. https://doi.org/10.3390/rs14194792

Anders, N., Valente, J., Masselink, R., & Keesstra, S. (2019). Comparing Filtering Techniques for Removing Vegetation from UAV-Based Photogrammetric Point Clouds. Drones, 3(3), 61. https://doi.org/10.3390/drones3030061

Axelsson, P. (2000) DEM generation from laser scanner data using adaptive TIN models. Int. Arch. Photogramm. Remote Sens. 33, 111-118.

Bartels, M. & Wei, H. (2006) Segmentation of LiDAR data using measures of distribution. Int. Arch. Photogramm., Remote Sens. Spatial Inf. Sci., vol. 36, no. 7, pp. 426-31.

Blistan, P., Kovanič, Ľ., Patera, M. & Hurčík, T. (2019) Evaluation quality parameters of DEM generated with low-cost UAV photogrammetry and Structure-from-Motion (SfM) approach for topographic surveying of small areas. Acta Montanistica Slovaca, Vol 24(3), 198-212.

Blistanova, M., Blistan, P. And Blazek, J. (2015) Mapping of surface objects and phenomena using Unmanned Aerial Vehicle for the purposes of crisis In Proceedings of the15th International Multidisciplinary Scientific GeoConference Surveying Geology and Mining Ecology Management. Sofia: STEF92 Technology, 2015, p. 491-500.

Blišťan, P., Kovanič, Ľ, Zelizňaková, V. & Palková, J. (2016) Using UAV photogrammetry to document rock outcrops. Acta Montanistica Slovaca, Volume 21, number 2, pp. 154-161, ISSN 1335-1788.

Braun, J., Braunová, H., Suk, T., Michal, O., Pěťovský, P. & Kurič, I. (2022). Structural and Geometrical Vegetation Filtering - Case Study on Mining Area Point Cloud Acquired by UAV Lidar. Acta Montanistica Slovaca, (26), 661-674. https://doi.org/10.46544/ams.v26i4.06

Buján, S., Cordero, M., & Miranda, D. (2020). Hybrid Overlap Filter for LiDAR Point Clouds Using Free Software. Remote Sensing, 12(7), 1051. https://doi.org/10.3390/rs12071051

Camargo Neto, J. A. (2004) Combined Statistical-Soft Computing Approach for Classification and Mapping Weed Species in Minimum-Tillage Systems. Ph.D. Thesis, ETD Collection for University of Nebraska, Lincoln, NE, USA; pp. 1-170.

Erdélyi, J., Kopáčik, A., & Kyrinovič, P. (2020). Spatial Data Analysis for Deformation Monitoring of Bridge Structures. Applied Sciences, 10(23), 8731. https://doi.org/10.3390/app10238731

Fawcett, T. (2006). An introduction to ROC analysis. Pattern Recognition Letters, 27(8), 861-874. https://doi.org/10.1016/j.patrec.2005.10.010

Guijarro, M., Pajares, G., Riomoros, I., Herrera, P., Burgos-Artizzu, X., & Ribeiro, A. (2011). Automatic segmentation of relevant textures in agricultural images. Computers and Electronics in Agriculture, 75(1), 75-83. https://doi.org/10.1016/j.compag.2010.09.013

Im, J., Jensen, J. R., & Hodgson, M. E. (2008). Object-Based Land Cover Classification Using High-Posting-Density LiDAR Data. GIScience & Remote Sensing, 45(2), 209-228. https://doi.org/10.2747/1548-1603.45.2.209

Jon, J., Koska, B., & Pospíšil, J. (2013). Autonomous Airship Equipped by Multi-Sensor Mapping Platform. The International Archives of the Photogrammetry, Remote Sensing and Spatial Information Sciences, XL-5/W1, 119-124. https://doi.org/10.5194/isprsarchives-xl-5-w1-119-2013

Keqi Zhang, Shu-Ching Chen, Whitman, D., Mei-Ling Shyu, Jianhua Yan, & Chengcui Zhang. (2003). A progressive morphological filter for removing nonground measurements from airborne LIDAR data. IEEE Transactions on Geoscience and Remote Sensing, 41(4), 872-882. https://doi.org/10.1109/tgrs.2003.810682

Kobler, A., Pfeifer, N., Ogrinc, P., Todorovski, L., Oštir, K., & Džeroski, S. (2007). Repetitive interpolation: A robust algorithm for DTM generation from Aerial Laser Scanner Data in forested terrain. Remote Sensing of Environment, 108(1), 9-23. https://doi.org/10.1016/j.rse.2006.10.013

Koska, B., & Křemen, T. (2013). The Combination of Laser Scanning and Structure from Motion Technology for Creation of Accurate Exterior and Interior Orthophotos of St. Nicholas Baroque Church. The International Archives Of The Photogrammetry, Remote Sensing And Spatial Information Sciences, XL-5/W1, 133-138. doi: 10.5194/isprsarchives-xl-5-w1-133-2013

Kovanič, Ľ., Blistan, P., Rozložník, M. and Szabó, G. (2021). UAS RTK / PPK photogrammetry as a tool for mapping the urbanized landscape, creating thematic maps, situation plans and DEM. Acta Montanistica Slovaca. Volume 26 (4) 649-660

Kovanič, U., Blistan, P., Štroner, M., Urban, R., & Blistanova, M. (2021). Suitability of Aerial Photogrammetry for Dump Documentation and Volume Determination in Large Areas. Applied Sciences, 11(14), 6564. https://doi.org/10.3390/app11146564

Kraus, K., & Pfeifer, N. (1998). Determination of terrain models in wooded areas with airborne laser scanner data. ISPRS Journal of Photogrammetry and Remote Sensing, 53(4), 193-203. https://doi.org/10.1016/s0924-2716(98)00009-4

Křemen, T. (2020). Measurement and Documentation of St. Spirit Church in Liběchov. In Advances and Trends in Geodesy, Cartography and Geoinformatics II; Taylor & Francis Group: London, UK, 2020; pp. 44-49. ISBN 978-0-367-34651-5. https://doi.org/10.1201/9780429327025.

Li, Y. (2013). Filtering Airborne Lidar Data by an Improved Morphological Method Based on Multi-Gradient Analysis. The International Archives of the Photogrammetry, Remote Sensing and Spatial Information Sciences, XL-1/W1, 191-194. https://doi.org/10.5194/isprsarchives-xl-1-w1-191-2013

Meyer, G.E., Hindman, T.W. & Laksmi, K. Machine Vision Detection Parameters for Plant Species Identification. In Proceedings of the Precision Agriculture and Biological Quality; International Society for Optics and Photonics, Boston, MA, USA, 14 January 1999; Volume 3543, pp. 327-335.

Moravec, D., Komárek, J., Kumhálová, J., Kroulík, M., Prošek, J. & Klápště, P. (2017). Digital Elevation Models as Predictors of Yield: Comparison of an UAV and Other Elevation Data Sources. Agronomy Research, 15: 249-255.

Moudrý, V., Lecours, V., Gdulová, K., Gábor, L., Moudrá, L., Kropáček, J., & Wild, J. (2018). On the use of global DEMs in ecological modelling and the accuracy of new bare-earth DEMs. Ecological Modelling, 383, 3-9. https://doi.org/10.1016/j.ecolmodel.2018.05.006

Moudrý, V., Moudrá, L., Barták, V., Bejček, V., Gdulová, K., Hendrychová, M., Šálek, M. (2021). The role of the vegetation structure, primary productivity and senescence derived from airborne LiDAR and hyperspectral data for birds diversity and rarity on a restored site. Landscape and Urban Planning, 210, 104064. https://doi.org/10.1016/j.landurbplan.2021.104064

Pavelka, K, Šedina, J., Matoušková, E, Hlaváčová, I. & Wilfried Korth (2019) Examples of different techniques for glaciers motion monitoring using InSAR and RPAS, European Journal of Remote Sensing, 52:sup1, 219-232, DOI: 10.1080/22797254.2018.1559001

Pingel, T. J., Clarke, K. C. & McBride, W. A. (2013). An improved simple morphological filter for the terrain classification of airborne LIDAR data. ISPRS Journal of Photogrammetry and Remote Sensing, 77, 21-30. https://doi.org/10.1016/j.isprsjprs.2012.12.002

Pukanská, K., Bartoš, K., Bella, P., Gašinec, J., Blistan, P., & Kovanič, U. (2020). Surveying and High-Resolution Topography of the Ochtiná Aragonite Cave Based on TLS and Digital Photogrammetry. Applied Sciences, 10(13), 4633. https://doi.org/10.3390/app10134633

Rizaldy, A., Persello, C., Gevaert, C., Oude Elberink, S., & Vosselman, G. (2018). Ground and Multi-Class Classification of Airborne Laser Scanner Point Clouds Using Fully Convolutional Networks. Remote Sensing, 10(11), 1723. https://doi.org/10.3390/rs10111723

Rybansky, M. (2022). Determination of Forest Structure from Remote Sensing Data for Modeling the Navigation of Rescue Vehicles. Applied Sciences, 12(8), 3939. https://doi.org/10.3390/app12083939

Sithole, G. (2001) Filtering of laser altimetry data using a slope adaptive filter. Int. Arch. Photogramm. Remote Sens. 34, 203-210.

Susaki, J. (2012). Adaptive Slope Filtering of Airborne LiDAR Data in Urban Areas for Digital Terrain Model (DTM) Generation. Remote Sensing, 4(6), 1804-1819. https://doi.org/10.3390/rs4061804

Štroner, M., Urban, R. & Línková, L. (2022) Multidirectional Shift Rasterization (MDSR) Algorithm for Effective Identification of Ground in Dense Point Clouds. Remote Sensing, 14, 4916. https://doi.org/10.3390/rs14194916

Štroner, M., Urban, R., & Línková, L. (2021). A New Method for UAV Lidar Precision Testing Used for the Evaluation of an Affordable DJI ZENMUSE L1 Scanner. Remote Sensing, 13(23), 4811. https://doi.org/10.3390/rs13234811

Štroner, M., Urban, R., Lidmila, M., Kolář, V., & Křemen, T. (2021). Vegetation Filtering of a Steep Rugged Terrain: The Performance of Standard Algorithms and a Newly Proposed Workflow on an Example of a Railway Ledge. Remote Sensing, 13(15), 3050. https://doi.org/10.3390/rs13153050

Torres-Sánchez, J., Mesas-Carrascosa, F. J., Jiménez-Brenes, F. M., de Castro, A. I., & López-Granados, F. (2021). Early Detection of Broad-Leaved and Grass Weeds in Wide Row Crops Using Artificial Neural Networks and UAV Imagery. Agronomy, 11(4), 749. https://doi.org/10.3390/agronomy11040749

Tovari, D. & Pfeifer, N. (2005) Segmentation based robust interpolation-A new approach to laser data filtering. Int. Arch. Photo-gramm. Remote Sens. Spat. Inf. Sci. 36, 79-84.

Urban, R., Štroner, M., Kuric, I. (2020). The use of onboard UAV GNSS navigation data for area and volume calculation. Acta Montanistica Slovaca, 25, 361-374. https://doi.org/10.46544/ams.v25i3.9

Vosselman, G. (2000) Slope based filtering of laser altimetry data. Int. Arch. Photogramm. Remote Sens. 33, 935-942.

Vosselman, G., Coenen, M., & Rottensteiner, F. (2017). Contextual segment-based classification of airborne laser scanner data. ISPRS Journal of Photogrammetry and Remote Sensing, 128, 354-371. https://doi.org/10.1016/j.isprsjprs.2017.03.010

Woebbecke, D. M., Meyer, G. E., Von Bargen, K. & Mortensen, D. A. (1995). Color Indices for Weed Identification Under Various Soil, Residue, and Lighting Conditions. Transactions of the ASAE, 38(1), 259-269. https://doi.org/10.13031/2013.27838

Zhang, J., Hu, X., Dai, H., & Qu, S. (2020). DEM Extraction from ALS Point Clouds in Forest Areas via Graph Convolution Network. Remote Sensing, 12(1), 178. https://doi.org/10.3390/rs12010178

Zhang, J., Lin, X., & Ning, X. (2013). SVM-Based Classification of Segmented Airborne LiDAR Point Clouds in Urban Areas. Remote Sensing, 5(8), 3749-3775. https://doi.org/10.3390/rs5083749

Zhang, W., Qi, J., Wan, P., Wang, H., Xie, D., Wang, X., & Yan, G. (2016). An Easy-to-Use Airborne LiDAR Data Filtering Method Based on Cloth Simulation. Remote Sensing, 8(6), 501. https://doi.org/10.3390/rs8060501